
ESTIMATE DEFORMATION CAPACITY OF NON-DUCTILE RC SHEAR WALLS USING EXPLAINABLE BOOSTING MACHINE

Zeynep Tuna Deger (1*), Gulsen Taskin Kaya (1), John W. Wallace (2)

(1) Istanbul Technical University, (2) University of California, Los Angeles

(*) corresponding author

{zeynep.tuna@itu.edu.tr, gulsen.taskin@itu.edu.tr, wallacej@ucla.edu}

Abstract

Machine learning is becoming increasingly prevalent for tackling challenges in earthquake engineering and providing fairly reliable and accurate predictions. However, it is mostly unclear how decisions are made because machine learning models are generally highly sophisticated, resulting in opaque black-box models. Machine learning models that are naturally interpretable and provide their own decision explanation, rather than using an explanatory, are more accurate in determining what the model actually computes. With this motivation, this study aims to develop a fully explainable machine learning model to predict the deformation capacity of non-ductile reinforced concrete shear walls based on experimental data collected worldwide. The proposed Explainable Boosting Machines (EBM)-based model is an interpretable, robust, naturally explainable glass-box model, yet provides high accuracy comparable to its black-box counterparts. The model enables the user to observe the relationship between the wall properties and the deformation capacity by quantifying the individual contribution of each wall property as well as the correlations among them. The mean coefficient of determination R^2 and the mean ratio of predicted to actual value based on the test dataset are 0.92 and 1.05, respectively. The proposed predictive model stands out with its overall consistency with scientific knowledge, practicality, and interpretability without sacrificing high accuracy.

Keywords: Explainable boosting machine, glass-box model, feature selection, general additive model, reinforced concrete shear wall, deformation capacity, interpretability

1 Introduction

Shear walls are typically utilized as the primary elements to resist lateral loads in reinforced concrete buildings. Towards capacity design assumptions, shear walls are designed to exhibit ductile behavior by providing adequate reinforcement and proper detailing. However, experimental studies have shown that walls with an aspect ratio smaller than 1.5 (i.e., squat walls) and those with poor reinforcement and detailing, despite their higher aspect ratio, end up showing brittle failure (e.g., diagonal tension, web crushing) [1, 2, 3]. Such walls are often observed in buildings not designed according to modern seismic codes and are prone to severe damage [4, 5]. As the performance-based design and assessment approach has gained importance concordant

with hazard mitigation efforts, there has been an increasing need and demand for reliable models to predict structural behavior under seismic actions. This objective is particularly important for walls that exhibit shear behavior as the nonlinear deformation capacity of such walls is assumed to be zero, potentially leading to technical and economical over-conservation. More realistic solutions can be achieved if their behavior is accurately estimated and considered in seismic performance evaluation.

The prediction of structural behavior has been achieved through the use of predictive equations or models that are developed based on available experimental data. Recently, machine learning (ML) methods have gained significant attention structural/earthquake engineering field and have demonstrated promising results despite the scarcity of data (compared to much larger data available in fields such as computer vision and image processing). Black-box models, with their high complexity and nonlinearity, often represent the input-output relationship better than the interpretable models in classification and regression applications. However, they are not necessarily consistent with true physical behavior. There are examples of misleading conclusions of black-box models in scientific and engineering applications [6, 7, 8]. Therefore, despite the high accuracy they achieve, black-box models are not completely accepted in earthquake engineering society. To leverage the advantages of the developments in artificial intelligence without ignoring the physical behavior, there has been recent research efforts that incorporates black-box machine learning methods with physical knowledge [8, 9, 10, 11]. This study takes this issue a step further and integrates an *explainable* machine learning approach (versus black-box) with existing physics-based understanding of seismic behavior to estimate the deformation capacity of non-ductile shear walls.

2 Literature Review

Research efforts in the literature to estimate wall deformation capacity have produced empirical models, some recently adopted by building codes [12]; however, they are relatively limited compared to other behavior features such as shear strength or failure mode. Earlier models were mainly developed using a limited number of experimental results [13, 14] or were trained using a single dataset; that is, they were not trained and tested based on unmixed data [12, 15]. Over time, as machine learning is embraced in the earthquake engineering field [16, 17, 18, 19, 20, 11] and new experiments are conducted, more advanced models have been developed. Yet, two main issues are encountered: (i) Some models used simple approaches such as linear regression for the sake of interpretability [21] and sacrificed overall accuracy (or had large dispersion). One might think that accurate models that predict relatively complicated behavior attributes can only be achieved by increasing model complexity; however, literature studies have shown that this may cause problems with the structure and distribution of the data [22, 23]. More importantly, urging the model to develop complex relationships to achieve higher performance typically leads to black-box models where internal mechanisms include highly nonlinear, complex relations. (ii) Such black-box models achieve high overall accuracy at the cost of explainability [18]. Researchers that acknowledge the significance of interpretability employed model-agnostic, local or global explanation methods (e.g., SHapley Additive exPlanation, Local Interpretable Model-agnostic Explanations) to interpret the decision mechanism of their models [11]. Such algorithms are not fully verified [24, 25]; besides, they are approximate approaches. Moreover, despite their broadening use and high accuracy, the black-box models are not entirely accepted in the earthquake engineering society as their internal relations are opaque and, in some cases, not entirely reliable [26]. Therefore, it is critical to understand how the model makes the decision/estimation to (i) verify that the model is physically meaningful, (ii) develop confidence in the predictive model, and (iii) broaden existing scientific knowledge with new insights. This study addresses this need and fills this important research gap by using domain-specific knowledge to evaluate and validate the decisions made by ML methods. Unlike the existing ML-based predictive models ([11, 18]), the proposed model aims particularly at the deformation capacity of non-ductile shear walls and is naturally transparent and interpretable.

Concerns regarding the trustworthiness and transparency of the black-box models motivated the development of a relatively new research area known as explainable artificial intelligence (XAI) [27, 28]. The XAI aims to provide a set of machine learning (ML) techniques for building more comprehensible and understandable models while maintaining a high level of learning performance. The strategies used in XAI are divided

into two main categories: explaining existing black-box models (post-hoc explainability) and generating glass-box (transparent) models. In the former, interpretability is confined to the usage of certain so-called explanatory algorithms that are employed to explain a black-box model, while in the latter, a predictive model is fully comprehensible and interpretable by humans. A model should have certain qualities to be considered a transparent model such as decomposability, algorithmic transparency, and simulatability [29]. The decomposability relates to the ability to explain each model component in terms of the inputs' contributions or correlations, whereas simulatability refers to the number of parameters (input) in the model representation (the less is the more understandable). The algorithmically transparent models enable a clear comprehension of the model' behavior for predicting any given output from its input data. Therefore, transparent models are highly needed approaches in fields where decisions are critical, but their performances are typically very low. Machine learning models that can maintain the tradeoff between performance and explainability, i.e., converging to the performance of black-box models while still providing explainability, would significantly address the demands in earthquake engineering society. In this context, explainable boosting machine (EBM) [30], a recently developed method belonging to the family of Generalized Additive Models (GAMs) [31], is a highly accurate and transparent ML method delivering an explicit and fully explainable predictive model. The EBM has been utilized in the literature to solve a variety of problems, including detecting common flaws in data [32], diagnosing COVID-19 using blood test variables [33], predicting diseases such as Alzheimer [34], or Parkinson [35], and has shown to outperform black-box models with the additional benefit of being an inherently explainable predictive model.

In this study, the EBM is used for the first time in the earthquake engineering field to construct an EBM-based predictive model for estimating deformation capacity on non-ductile RC shear walls. The inputs of the predictive model are designated as the shear wall design properties (e.g., wall geometry, reinforcing ratio), whereas the output is one of the constitutive components of the nonlinear wall behavior, that is, the deformation capacity. The main contributions of this research are highlighted as follows:

- A fully transparent and interpretable predictive model is developed to estimate the deformation capacity of RC shear walls that are failed in pure shear or shear-flexure interaction.
- The proposed model meets all desired properties, i.e., decomposability, algorithmic transparency, and simulatability, without compromising high performance.
- This study integrates novel computational methods (i.e., EBM) and domain-based knowledge to formalize complex engineering knowledge. The proposed model's overall consistency with a physics-based understanding of seismic behavior is verified.

3 The RC Shear Wall Database

The experimental data used in this research is a sub-assembly of the wall test database utilized in Deger and Taskin (2022) [19] with 30 additional data [36, 37]. As the main focus is to estimate the deformation capacity of walls governed by shear or shear-flexure interaction, walls that did not show so-called shear failure indications are excluded from the database, resulting in 286 specimens of use for this research. All specimens were tested under quasi-static cyclic loading, whereas none was retrofitted and re-tested. The database consists of wall design parameters, which are herein designated as the input variables of the machine learning problem, namely: wall geometry (t_w , l_w , h_w), shear span ratio (M/Vl_w), concrete compressive strength (f_c), longitudinal and transverse reinforcing ratios at web (f_{yl} , f_{yt}), longitudinal and transverse reinforcing ratios at boundary elements (f_{ybl} , f_{ysh}), axial load ratio ($P/A_g f_c$), shear demand (or strength) at the section (V_{max}), cross-section type (rectangular, barbell-shape, or flanged), curvature type (single or double). It is noted that single curvature and double curvature correspond to the end conditions of the specimen, i.e., cantilever and fixed-fixed, respectively. Distributions of the input variables are presented in Fig.1 along with their box plots (shown in blue).

The output variable of the ML problem, the deformation capacity, is taken directly as the reported ultimate displacement prior to its failure if the specimen is tested until failure. Otherwise, it is assumed as the displacement corresponding to $0.8V_{max}$ as suggested by Park, 1989. It is noted that failure displacement

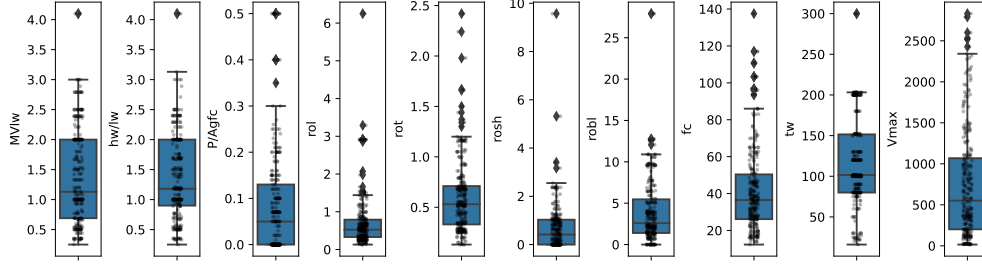


Figure 1: Distribution of the input variables in the database.

was taken as the total wall top displacement and was not separated into shear and flexural deformation components.

4 Explainable Boosting Machines

Explainable Boosting Machines (EBM) is a state-of-the-art machine learning technique designed as accurately as random forests and boosted trees while also being simple to understand [30, 38]. The EBM delivers a complete explainable learning model that belongs to the family of Generalized Additive Models (GAMs) [39]:

$$g(f(x_1, \dots, x_n)) = f_0 + f_1(x_1) + f_2(x_2) + \dots, f_n(x_n) \quad (1)$$

where f_0 is an intercept, and each f_j is called a shape function, representing the individual effect of the x_j -th variable on the model output, $f(x_1, \dots, x_n)$. The g is utilized as a link function, adapting the model to different settings, e.g., identity function for regression and logistic function for classification. The intercept, f_0 , is calculated as the mean response of all the outputs. Because the shape functions are trained independently for each input variable, the model is additive (decomposable), allowing to separately analyze the effect of each input variable on the model output. The EBM is designed to improve the performance of the standard GAM while maintaining its interpretability.

Generalized Additive Models are more comprehensible than black-box models, but the analytical form of the shape functions is typically unknown, making it unsuitable for machine learning purposes. Although other analytical functions, such as splines or orthogonal polynomials, can be offered for defining shape functions, they are frequently less accurate when representing a nonlinear model [40]. The EBM uses shallow trees to construct the shape functions; therefore, it easily captures the nonlinearity of the data. Each input variable (x_i) is modeled with ensemble trees such as bagging and gradient boosting. As a result, rather than employing the spline method, which is prevalent in traditional GAMs, the function associated with each input variable or interaction is produced from a vast set of shallow trees.

The EBM offers both local and global explanations of the learning model as each variable importance is estimated as the average absolute value of the predicted score. Moreover, each shape function can be visualized (algorithmically transparent); therefore, it is possible to observe the effects of the particular feature at certain intervals. In the inference phase, all the terms in Eq.1 are added up and passed through the link function to g to compute the final prediction as shown in Fig. 2. In other words, individual predictions are generated using the shape functions, f_i , which act as a lookup table.

To demonstrate which feature had the largest impact on the individual forecast, the contributions can be sorted and shown using the principles of additivity and modularity.

The EBM's performance can be improved by including pairwise effects between variables in the model representation. For better performance, additional interactions can be incorporated; however, this may result in a more complex model with lower generalization performance due to the increased number of model parameters to be trained. The pairwise interactions are included in GA²Ms [41], which is a second-order

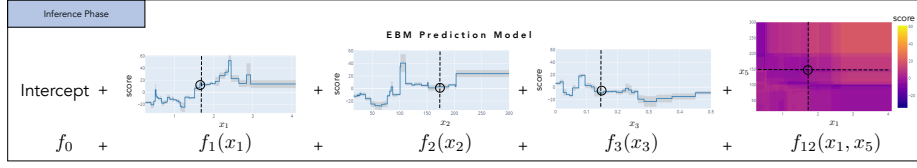


Figure 2: Inference phase of EBM.

additive model:

$$g(E[y]) = f_0 + \sum_{i=1}^n f_i(x_i) + \sum_{i=1}^K f_k(x_{k_1}, x_{k_2}) \quad (2)$$

where K pairs of features (k_1, k_2) are chosen greedily (FAST algorithm) [42]. The pairwise interaction $f_{ij}(x_i, x_j)$ could be rendered as a heatmap on the two-dimensional x_i, x_j - plane, still providing high intelligibility. Even though adding more interactions does not affect the model’s explainability, the final prediction model may be less comprehensible due to a large number of interactions (less simulatability).

5 Development of the Predictive Model

5.1 Overall Performance of EBM

To assess whether the method compromises accuracy for the sake of interpretability, the performance of the EBM model is compared to three state-of-the-art black-box machine learning models, namely: XGBoost [43], Gradient Boost [44], Random Forest [45], and two glass-box models, namely Ridge Linear Regression [46], Decision Tree [47]. All the implementations are carried out in a Python environment. For all ML models, the entire database, including all twelve input variables (ten variables from Fig.1 and two binary coded variables for curvature type and cross-section type), is randomly split into training and test datasets with a ratio of 90% and 10%, respectively.

Tunning of the hyperparameters, such as learning rate, number of leaves, number of interactions, and so on, typically affects the performance of the corresponding regression model. For hyperparameter tuning, a 10-fold cross-validation technique (Fig. 3) is used, wherein a subset of the data is kept as validation data, and the model’s performance is evaluated using various hyperparameter settings on the validation set. This method prevents the tuning from overfitting the training dataset.

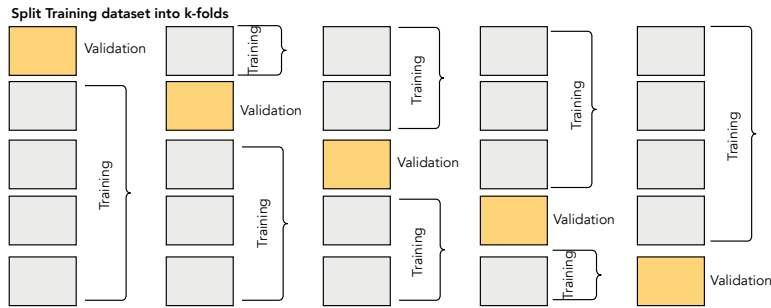


Figure 3: Illustration of k-fold cross-validation technique, where k is set to 5.

For performance evaluations, the following three metrics are used over “unseen” (i.e., not used in the training process) test data sets of ten random train-test data splittings: coefficient of determination (R^2), relative

Table 1: Mean performance scores based on the test datasets over ten random splittings.

	Black-box			Glass-box		
	EBM	XGBoost	GB	RF	RLR	DT
R²	0.83	0.80	0.79	0.83	0.41	0.67
RE (%)	0.41	0.40	0.32	0.28	0.67	0.47
PA	1.21	1.17	1.20	1.15	2.0	1.9

error (RE), and prediction accuracy (PA), as given in Eqs. 3, 4, and 5, respectively.

$$R^2 = 1 - \frac{\sum_i (y_i - \hat{y}_i)^2}{\sum_i (y_i - \bar{y})^2} \quad (3)$$

$$RE = \frac{\sum_i |\hat{y}_i - y_i|}{\sum_i |y_i|} \times 100\% \quad (4)$$

$$PA = \sum_i \frac{y_i}{\hat{y}_i} \quad (5)$$

where y_i , \bar{y} , \hat{y}_i , and m refer to the actual output, the mean value of y_i s, predicted output of corresponding regression model, and a number of samples in the test dataset, respectively.

Mean performance scores of the ML models are summarized in Table 1, along with their dispersion demonstrated in box plots in Fig. 4. The results indicate that EBM achieves comparable performance with its black-box counterparts, with a correlation of determination of $R^2 = 0.83$, a relative error of 0.41%, and a $PA = 1.21$. As seen in Fig. 4, the low R^2 , RE , and PA deviations of EBM imply that reliable predictions can be achieved regardless of the selected train-test splitting and verify the model's robustness. Mean prediction accuracy (PA) shows around 20% of overestimation for EBM and the black-box methods, suggesting that some input variables are potentially noisy. Compared to transparent models, the EBM outperforms both the Decision Tree (DT) and Ridge Linear Regression (RLR) across all three metrics, indicating that it is far superior to the traditional glass-box approaches.

The most remarkable advantage of the EBM method over the others is that it provides full explainability without sacrificing accuracy. Unlike other methods, EBM enables the user to understand how the prediction is made and which parameters are essential in the decision-making process. Therefore, the EBM method is selected as the baseline algorithm for the rest of the analysis to propose a prediction model for estimating the deformation capacity based on the following criteria: developing a model with fewer input variables (high simulatability), achieving high accuracy, and ensuring physical consistency.

5.2 The Proposed EBM-based Predictive Model

The importance of the wall properties in predicting the deformation capacity is evaluated based on additive term contributions visualized in Fig.5. Results reveal that t_w and M/Vl_w (or h_w/l_w) have the greatest impact on individual predictions. This is consistent with the mechanics of the behavior as walls with smaller thickness are shown to be more susceptible to lateral stiffness degradation due to concrete spalling, leading to a failure caused by lateral instabilities or out-of-plane buckling [48, 49]. The shear span ratio (or aspect ratio), on the other hand, both have a significant impact on deformation capacity as the higher the shear span ratio gets, the slender the wall is, and the higher deformations it typically can reach prior to its failure. The least important wall parameters, on the other hand, are identified as curvature type, cross-section type, and concrete compressive strength.

Another critical aspect considered in this study is to develop the predictive model with as few input variables as possible. With that, the computational workload is aimed to be reduced, and a more practical and interpretable model is proposed for potential users. To achieve this, knowledge-based-selected combinations

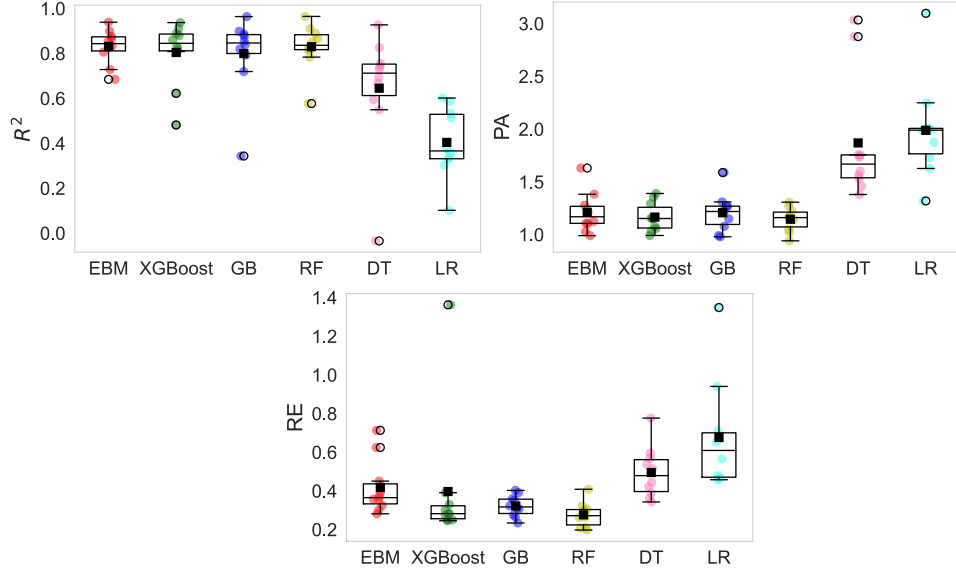


Figure 4: Comparison of performance scores of ML methods for test samples based on ten random train splittings.

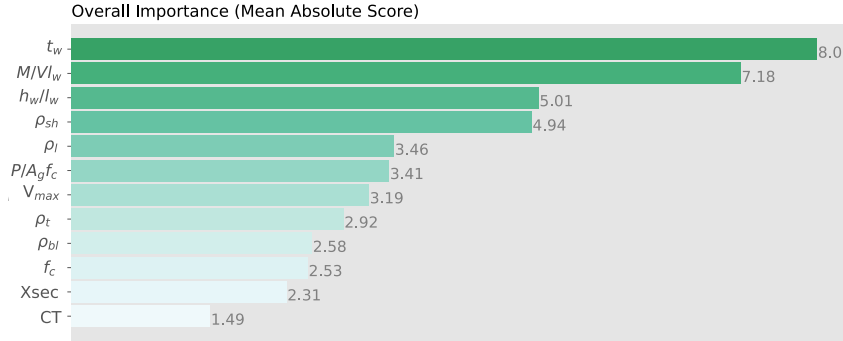


Figure 5: EBM Global interpretation for twelve features included

of four-to-five features are exhaustively evaluated to reach performance scores as high as when twelve features are included.

EBM can achieve similar performance scores using four features: M/Vl_w , $P/A_g f_c$, t_w , and V_{max} . Including additional features (e.g., ρ_l , ρ_{bl} , ρ_{sh}) deemed impactful by EBM as well as experimental results [50, 51] has only a modest effect on the overall performance. The performances of other methods are close to their benchmark model (including twelve features), whereas the glass-box methods are affected by the reduction of input size and show much lower performances. The mean R^2 drops to 0.33 for the Ridge Linear Regression, imparting that the input-output relation is not linear.

The proposed EBM-based predictive model is selected to achieve the highest R^2 with a prediction accuracy as close to 1.0 as possible. The correlation plots are presented in Fig. 6 for training and test data sets, where

scattered data are concentrated along the $y = x$ line, demonstrating that the proposed model can make accurate predictions. It should be noted that the distribution of the residuals is concentrated around zero.

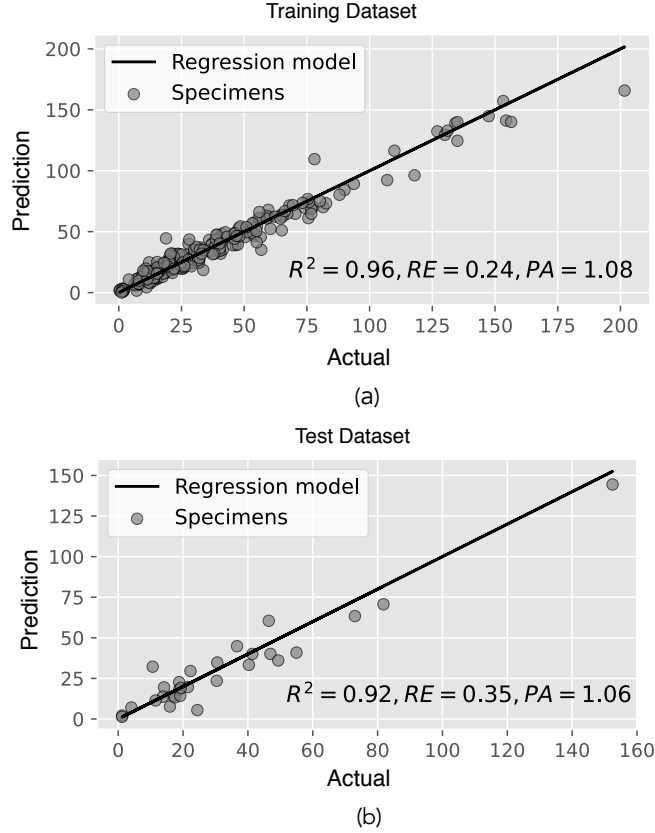


Figure 6: Correlations of the model outputs with the actual values for (a) training and (b) test datasets

As discussed above, the proposed model is an additive model in which each relevant feature is designated a quantitative term contribution. The EBM allows the user to explore the contribution of each feature to the model by plotting their shape functions (Fig.7a-d). As discussed above, the EBM method employs multiple decision-tree learning models; therefore, inclines and declines are undertaken with jump-looking piece-wise constant functions (versus smooth curves). The values, called scores, are read from these functions, and those from heat maps (Fig.7e-f) representing pairwise interactions (i.e., between two features) are summed up to calculate the prediction. The gray zones along the shape functions designate error bars that indicate the model's uncertainty and data sensitivity. This typically occurs in cases of sparsity or the presence of outliers within the associated region.

The shape functions in Fig.7 also indicate their correlations with the output in a graphical representation. For example, nonlinear patterns that can not be observed in linear approaches can be easily interpreted [52], which provides new insights to broaden existing experimental-based knowledge. For example, the shear demand V_{max} (Fig.7d) reduces ductility; thus deformation capacity, as demonstrated by experimental results [53] and suggested by ASCE 41-17 acceptance criteria. Yet, a highly nonlinear pattern is observed when relevant experimental data are gathered [11, 21]. This nonlinearity can be observed in the shape function suggested by the proposed method. Other input variables (t_w , $P/A_g f_c$, M/Vl_w), on the other hand, demonstrate an almost-linear trend. The interpretation of EBM for these variables is consistent with experimental results

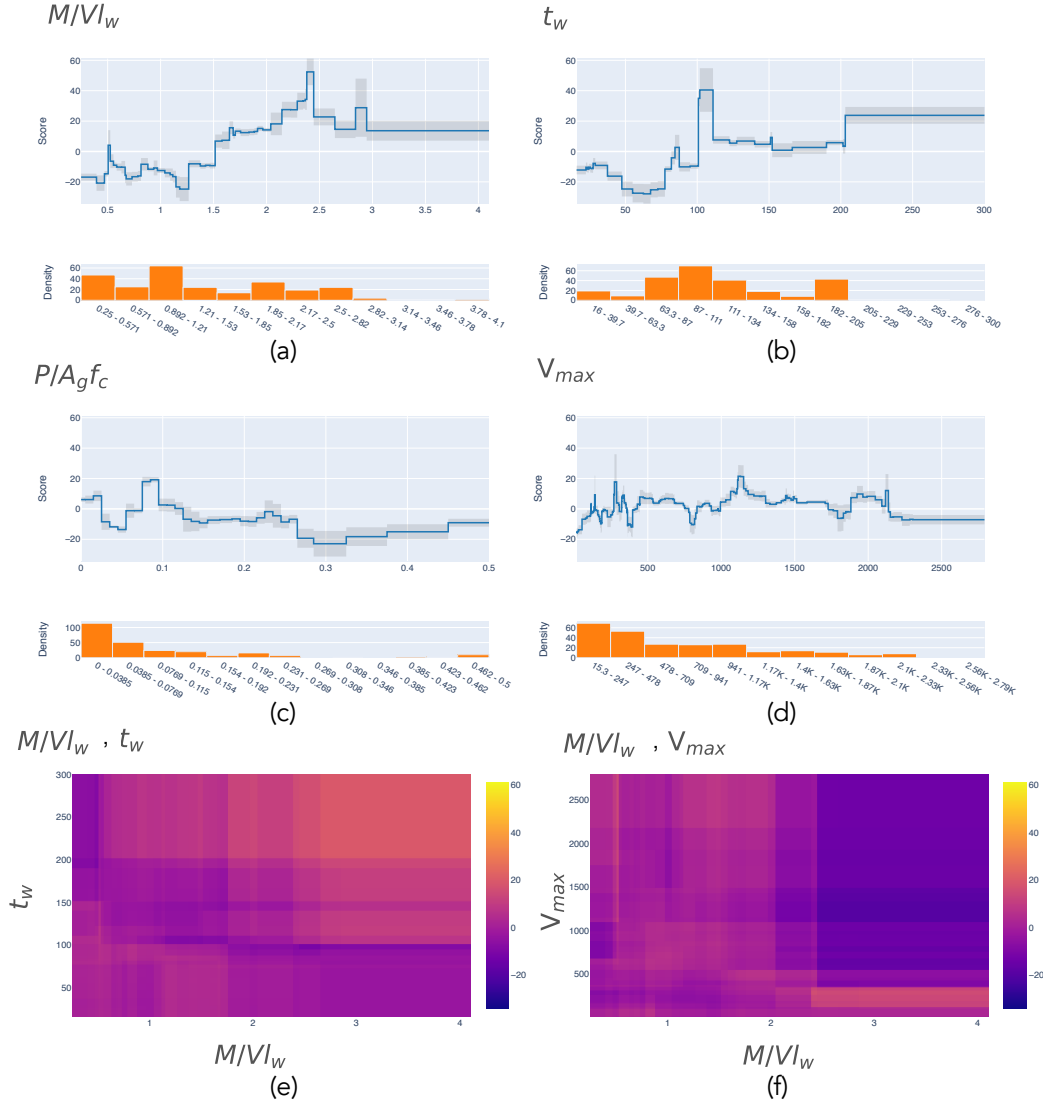


Figure 7: EBM shape functions (a-d) and pairwise interaction plots (e-f) for the proposed model. Note that the intercept $f_0 = 35.528$.

in the literature, such that M/Vl_w (Fig.7a) and t_w (Fig.7b) have a positive impact, as discussed above, whereas $P/A_g f_c$ (Fig.7c) has an adverse influence [54, 55]. The reason for M/Vl_w and t_w (Fig.7b) suggesting an inverse effect up to a certain point ($M/Vl_w \approx 1.2$, $t_w \approx 60$ cm, $P/A_g f_c \approx 0.08$) is because the model has an intercept value (f_0 , Eq.2) and specimens with smaller deformation capacities (f_0 less than 35.528) are predicted adding up negative values. The unexpected jumps in t_w are likely because there is an abrupt accumulation of data at $t_w = 100$ mm and $t_w = 200$ mm (64 and 44 specimens, respectively), which probably causes difficulty in decision making.

It is noted that the EBM method offers controllability over the structure of the model proposed by, for instance, modifying the number of pairwise interactions. This allows the method to suggest more than one

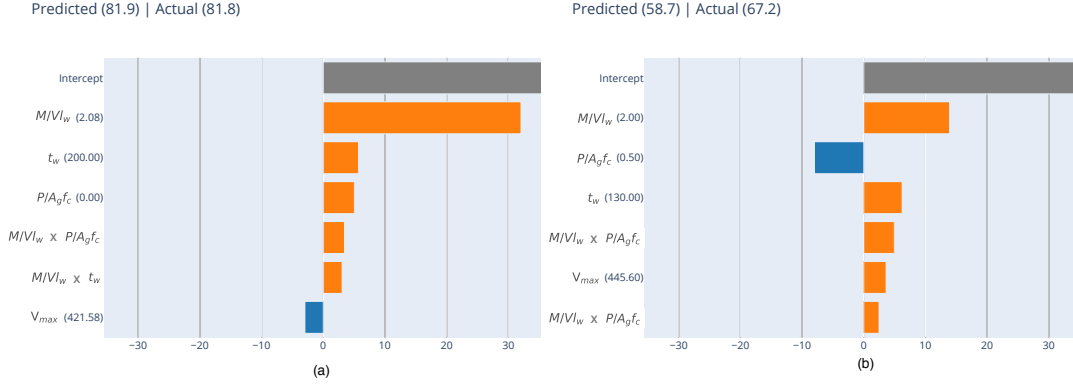


Figure 8: Variable contribution estimates for (a) well-predicted, (b) averagely-predicted samples.

model for the same input-output configuration for a particular train-test dataset. Reducing the number of interactions brings simplicity to the model; however, it typically loses accuracy as EBM relies on its automatically-determined interactions in the decision-making process. Given this trade-off, the number of interactions is set to two for the proposed model.

5.3 Sample-Based Explanation

This section presents the prediction of deformation capacity for two example specimens using the proposed EBM-based predicted model. One specimen is predicted with excellent accuracy (almost zero error; Fig.8a), whereas the other is predicted with around 15% error (Fig.8b).

Variable contribution estimates for each specimen are presented such that the intercept is constant and shown in gray, the additive terms with positive impact are marked in orange, and additive terms decreasing the output are shown in blue. Each contribution estimate is extracted from the shape functions and two-dimensional heat maps (Fig.7) based on the input values of a specific specimen. Overall, the model is consistent with physical knowledge, except V_{max} has an unexpected positive impact on the output for the relatively worse prediction (Fig.8b). This is an excellent advantage of EBM; that is, the user can prudently understand how the prediction is made for a new sample and develop confidence in the predictive model (versus blind acceptance in black-box models).

5.4 Comparisons with Current Code Provisions

ASCE 41-17 and ACI 369-17 [56] provide recommended deformation capacities for nonlinear modeling purposes, where shear walls are classified into the following two categories based on their aspect ratio: shear-controlled ($h_w/l_w > 1.5$) and flexure-controlled ($h_w/l_w > 3.0$). The deformation capacity of shear-controlled walls is identified as drift ratio such that $\Delta_u/h_w = 1.0$ if the wall axial load level is greater than 0.5 and $\Delta_u/h_w = 2.0$ otherwise.

Deformation capacity predictions based on the proposed EBM model are compared to ASCE 41-17/ACI 369-17 provisions in Fig. 9. Predicted-to-actual ratios are 1.06 ± 0.49 and 6.42 ± 3.17 for EBM-based model and code predictions, respectively. The results imply that traditional approaches may lead to the overestimation of deformation capacities and cause unsafe assessments.

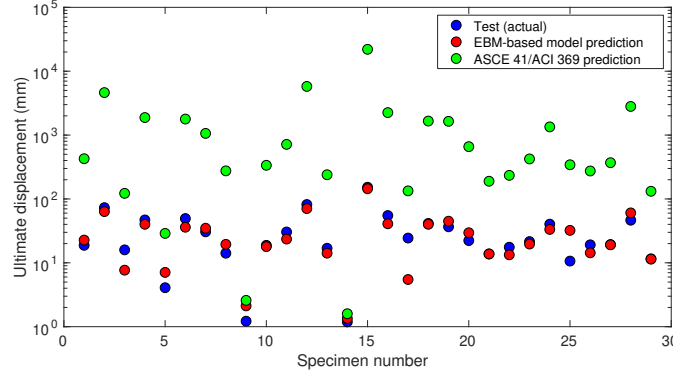


Figure 9: Comparisons of EBM-based model predictions with code provisions.

6 Conclusions

A fully transparent predictive model is developed to estimate the deformation capacity of reinforced concrete shear walls that are failed in pure shear or shear-flexure interaction. To achieve this, a state-of-the-art machine learning method, Explainable Boosting Machines (EBM), designed as accurately as random forests and boosted trees, is utilized. The EBM provides an additive model such that each relevant feature is designated a quantitative term contribution. The input-output configuration of the model is designated as the shear wall design properties (e.g., wall geometry, axial load ratio) and ultimate wall displacement, respectively. The conclusions derived from this study are summarized as follows:

- The importance of the wall properties in predicting the deformation capacity is evaluated based on additive term contributions. t_w and M/Vl_w (or h_w/l_w) have the greatest effect on individual predictions, whereas the least relevant ones are identified as curvature type, cross-section type, and concrete compressive strength.
- Compared to three black-box models (XGBoost, Gradient Boost, Random Forest), the EBM achieves similar or better performance in terms of correlation of determination (R^2), relative error (RE), and prediction accuracy (PA ; the ratio of predicted to the actual value). The EBM achieves a mean R^2 of 0.83 and a mean RE of 0.41% using twelve input variables based on ten random train-test splittings.
- Compared to two glass-box methods (Decision Tree (DT) and Ridge Linear Regression (RLR)), the EBM outperforms both methods across all three metrics.
- The dispersion of performance metrics of EBM is small, implying that the model is robust and the performance is relatively less data-dependent.
- Compared to the developed model when all the available features are used, the EBM achieves competitive performance scores using only four input variables: M/Vl_w , $P/A_g f_c$, t_w , and V_{max} . Using these four features, the proposed EBM-based model achieves R^2 of 0.92 and PA of 1.05 based on the test dataset. Using fewer variables ensures that the model is less simulatable, more practical, more comprehensible, and reduces the computational cost.
- It is important to note that the decision-making process developed by the proposed EBM-based model has overall consistency with scientific knowledge despite several exceptions detected in sample-based inferences. This is an excellent advantage of the proposed model; that is, the user can assess and evaluate the prediction process before developing confidence in the result (versus blindly accepting as in black-box models).

- This model delivers exact intelligibility, i.e., there is no need to use local explanation methods (e.g., SHAP, LIME) to interpret the learning model, which obviates the uncertainties associated with their approximations.

The proposed EBM-based model is valuable in that it is simultaneously accurate, explainable, and consistent with scientific knowledge. The EBM's ability to provide interpretable and transparent results would allow engineers to better understand the factors that affect the deformation capacity of non-ductile RC shear walls and make informed design decisions. The use of the EBM to estimate deformation capacity would improve the reliability and efficiency of structural analysis and design processes, leading to safer and more cost-effective buildings.

References

- [1] ASCE-41. *ASCE Standard, ASCE/SEI, 41-17, Seismic Evaluation and Retrofit of Existing Buildings*. American Society of Civil Engineers, 2017.
- [2] Leonardo M Massone and John W Wallace. Load-deformation responses of slender reinforced concrete walls. *Structural Journal*, 101(1):103–113, 2004.
- [3] Chadchart Sittipunt, Sharon L Wood, Panitan Lukkunaprasit, and Pichai Pattararattanakul. Cyclic behavior of reinforced concrete structural walls with diagonal web reinforcement. *Structural Journal*, 98(4):554–562, 2001.
- [4] John W Wallace, Leonardo M Massone, Patricio Bonelli, Jeff Dragovich, René Lagos, Carl Lüders, and Jack Moehle. Damage and implications for seismic design of rc structural wall buildings. *Earthquake Spectra*, 28(1_suppl1):281–299, 2012.
- [5] C Arnold, B Bolt, D Dreger, E Elsesser, R Eisner, W Holmes, G McGavin, and C Theodoropoulos. Fema 454: Design for earthquakes: A manual for architects, 2006.
- [6] David Lazer, Ryan Kennedy, Gary King, and Alessandro Vespignani. The parable of google flu: traps in big data analysis. *Science*, 343(6176):1203–1205, 2014.
- [7] John Douglas and Hideo Aochi. A survey of techniques for predicting earthquake ground motions for engineering purposes. *Surveys in geophysics*, 29(3):187–220, 2008.
- [8] Anuj Karpatne, Ramakrishnan Kannan, and Vipin Kumar. *Knowledge Guided Machine Learning: Accelerating Discovery using Scientific Knowledge and Data*. CRC Press, 2022.
- [9] Huan Luo and Stephanie German Paal. Artificial intelligence-enhanced seismic response prediction of reinforced concrete frames. *Advanced Engineering Informatics*, 52:101568, 2022.
- [10] Siyang Zhou, Shanglin Liu, Yilan Kang, Jie Cai, Haimei Xie, and Qian Zhang. Physics-based machine learning method and the application to energy consumption prediction in tunneling construction. *Advanced Engineering Informatics*, 53:101642, 2022.
- [11] Muneera A Aladsani, Henry Burton, Saman A Abdullah, and John W Wallace. Explainable machine learning model for predicting drift capacity of reinforced concrete walls. *ACI Structural Journal*, 119(3), 2022.
- [12] Saman A Abdullah and John W Wallace. Drift capacity of reinforced concrete structural walls with special boundary elements. *ACI Structural Journal*, 116(1):183, 2019.
- [13] T Paulay, MJN Priestley, and AJ Synge. Ductility in earthquake resisting squat shearwalls. In *Journal Proceedings*, volume 79, pages 257–269, 1982.
- [14] İlker Kazaz, Polat Gülkan, and Ahmet Yakut. Deformation limits for structural walls with confined boundaries. *Earthquake Spectra*, 28(3):1019–1046, 2012.
- [15] Sofia Grammatikou, Dionysis Biskinis, and Michael N Fardis. Strength, deformation capacity and failure modes of rc walls under cyclic loading. *Bulletin of earthquake engineering*, 13(11):3277–3300, 2015.
- [16] Sujith Mangalathu, Hansol Jang, Seong-Hoon Hwang, and Jong-Su Jeon. Data-driven machine-learning-based seismic failure mode identification of reinforced concrete shear walls. *Engineering Structures*, 208:110331, 2020.
- [17] De-Cheng Feng, Wen-Jie Wang, Sujith Mangalathu, and Ertugrul Taciroglu. Interpretable xgboost-shap machine-learning model for shear strength prediction of squat rc walls. *Journal of Structural Engineering*, 147(11):04021173, 2021.
- [18] Haoyou Zhang, Xiaowei Cheng, Yi Li, and Xiuli Du. Prediction of failure modes, strength, and deformation capacity of rc shear walls through machine learning. *Journal of Building Engineering*, 50:104145, 2022.
- [19] Zeynep Tuna Deger and Gulsen Taskin. A novel gpr-based prediction model for cyclic backbone curves of reinforced concrete shear walls. *Engineering Structures*, 255:113874, 2022.

- [20] Zeynep Tuna Deger and Gulsen Taskin Kaya. Glass-box model representation of seismic failure mode prediction for conventional reinforced concrete shear walls. *Neural Computing and Applications*, pages 1–13, 2022.
- [21] Zeynep Tuna Deger and Cagri Basdogan. Empirical expressions for deformation capacity of reinforced concrete structural walls. *ACI Structural Journal*, 116(6), 2019.
- [22] Justin M Johnson and Taghi M Khoshgoftaar. Survey on deep learning with class imbalance. *Journal of Big Data*, 6(1):1–54, 2019.
- [23] Bhavya Kailkhura, Brian Gallagher, Sookyoung Kim, Anna Hiszpanski, and T Han. Reliable and explainable machine-learning methods for accelerated material discovery. *npj Computational Materials*, 5(1):1–9, 2019.
- [24] I Elizabeth Kumar, Suresh Venkatasubramanian, Carlos Scheidegger, and Sorelle Friedler. Problems with shapley-value-based explanations as feature importance measures. In *International Conference on Machine Learning*, pages 5491–5500. PMLR, 2020.
- [25] Cynthia Rudin. Stop explaining black box machine learning models for high stakes decisions and use interpretable models instead. *Nature Machine Intelligence*, 1(5):206–215, 2019.
- [26] Christoph Molnar. *Interpretable machine learning*. Lulu. com, 2020.
- [27] Amina Adadi and Mohammed Berrada. Peeking inside the black-box: a survey on explainable artificial intelligence (xai). *IEEE access*, 6:52138–52160, 2018.
- [28] Zachary C Lipton. The mythos of model interpretability: In machine learning, the concept of interpretability is both important and slippery. *Queue*, 16(3):31–57, 2018.
- [29] Alejandro Barredo Arrieta, Natalia Díaz-Rodríguez, Javier Del Ser, Adrien Bennetot, Siham Tabik, Alberto Barbado, Salvador García, Sergio Gil-López, Daniel Molina, Richard Benjamins, et al. Explainable artificial intelligence (xai): Concepts, taxonomies, opportunities and challenges toward responsible ai. *Information fusion*, 58:82–115, 2020.
- [30] Harsha Nori, Samuel Jenkins, Paul Koch, and Rich Caruana. Interpretml: A unified framework for machine learning interpretability. *arXiv preprint arXiv:1909.09223*, 2019.
- [31] Trevor Hastie, Robert Tibshirani, and Jerome Friedman. Additive models, trees, and related methods. In *The Elements of Statistical Learning*, pages 295–336. Springer, 2009.
- [32] Zhi Chen, Sarah Tan, Harsha Nori, Kori Inkpen, Yin Lou, and Rich Caruana. Using explainable boosting machines (ebms) to detect common flaws in data. In *Joint European Conference on Machine Learning and Knowledge Discovery in Databases*, pages 534–551. Springer, 2021.
- [33] Lucas M Thimoteo, Marley M Vellasco, Jorge Amaral, Karla Figueiredo, Cátia Lie Yokoyama, and Erito Marques. Explainable artificial intelligence for covid-19 diagnosis through blood test variables. *Journal of Control, Automation and Electrical Systems*, 33(2):625–644, 2022.
- [34] Alessia Sarica, Andrea Quattrone, and Aldo Quattrone. Explainable boosting machine for predicting alzheimer’s disease from mri hippocampal subfields. In *International Conference on Brain Informatics*, pages 341–350. Springer, 2021.
- [35] Alessia Sarica, Andrea Quattrone, and Aldo Quattrone. Explainable machine learning with pairwise interactions for the classification of parkinson’s disease and swedd from clinical and imaging features. *Brain Imaging and Behavior*, pages 1–11, 2022.
- [36] R Tokunaga and T Nakachi. Experimental study on edge confinement of reinforced concrete core walls. In *Fifteenth World Conference on Earthquake Engineering, Lisbon*, pages 1–5, 2012.
- [37] Masaya Hirose. Past experimental results on reinforced concrete shear walls and analysis on them. *Kenchiku Kenkyu Shiryo*, 6:33–34, 1975.
- [38] Harsha Nori, Rich Caruana, Zhiqi Bu, Judy Hanwen Shen, and Janardhan Kulkarni. Accuracy, interpretability, and differential privacy via explainable boosting. In *International Conference on Machine Learning*, pages 8227–8237. PMLR, 2021.

- [39] Trevor Hastie and Robert Tibshirani. Generalized additive models: some applications. *Journal of the American Statistical Association*, 82(398):371–386, 1987.
- [40] Mathew W McLean, Giles Hooker, Ana-Maria Staicu, Fabian Scheipl, and David Ruppert. Functional generalized additive models. *Journal of Computational and Graphical Statistics*, 23(1):249–269, 2014.
- [41] Yin Lou, Rich Caruana, and Johannes Gehrke. Intelligible models for classification and regression. In *Proceedings of the 18th ACM SIGKDD international conference on Knowledge discovery and data mining*, pages 150–158, 2012.
- [42] Simon N Wood. Fast stable direct fitting and smoothness selection for generalized additive models. *Journal of the Royal Statistical Society: Series B (Statistical Methodology)*, 70(3):495–518, 2008.
- [43] Tianqi Chen and Carlos Guestrin. Xgboost: A scalable tree boosting system. In *Proceedings of the 22nd acm sigkdd international conference on knowledge discovery and data mining*, pages 785–794, 2016.
- [44] Jerome H Friedman. Greedy function approximation: a gradient boosting machine. *Annals of statistics*, pages 1189–1232, 2001.
- [45] Leo Breiman. Random forests. *Machine learning*, 45(1):5–32, 2001.
- [46] Trevor Hastie, Robert Tibshirani, Jerome H Friedman, and Jerome H Friedman. *The elements of statistical learning: data mining, inference, and prediction*, volume 2. Springer, 2009.
- [47] Leo Breiman, Jerome H Friedman, Richard A Olshen, and Charles J Stone. *Classification and regression trees*. Routledge, 2017.
- [48] Jose Miguel Vallenias, Vitelmo Victorio Bertero, and Egor Paul Popov. Hysteric behavior of reinforced concrete structural walls. *NASA STI/Recon Technical Report N*, 80:27533, 1979.
- [49] RG Oesterle, AE Fiorato, LS Johal, JE Carpenter, HG Russell, and WG Corley. Earthquake resistant structural walls-tests of isolated walls. *Research and Development Construction Technology Laboratories, Portland Cement Association*, 1976.
- [50] AA Tasnimi. Strength and deformation of mid-rise shear walls under load reversal. *Engineering Structures*, 22(4):311–322, 2000.
- [51] MA Hube, A Marihuén, Juan Carlos de la Llera, and Bozidar Stojadinovic. Seismic behavior of slender reinforced concrete walls. *Engineering Structures*, 80:377–388, 2014.
- [52] Patrick Zschech, Sven Weinzierl, Nico Hambauer, Sandra Zilker, and Mathias Kraus. Gam (e) changer or not? an evaluation of interpretable machine learning models based on additive model constraints. *arXiv preprint arXiv:2204.09123*, 2022.
- [53] WG Corley, AE Fiorato, and RG Oesterle. Structural walls. *Special Publication*, 72:77–132, 1981.
- [54] Ioannis D Lefas, Michael D Kotsovos, and Nicholas N Ambraseys. Behavior of reinforced concrete structural walls: strength, deformation characteristics, and failure mechanism. *Structural Journal*, 87(1):23–31, 1990.
- [55] Firooz Emamy Farvashany, Stephen J Foster, and B Vijaya Rangan. Strength and deformation of high-strength concrete shearwalls. *ACI structural journal*, 105(1):21, 2008.
- [56] ACI Committee 369. *Standard Requirements for Seismic Evaluation and Retrofit of Existing Concrete Buildings (ACI 369-17) and Commentary*. ACI (American Concrete Institute), Farmington Hills, MI, 2017.